



# Interaction investigation of single and multiple carbon monoxide molecules with Fe-, Ru-, and Os-doped single-walled carbon nanotubes by DFT study: applications to gas adsorption and detection nanomaterials

Chanukorn Tabtimsai<sup>1</sup> · Wandee Rakrai<sup>1</sup> · Suphawarat Phalinyot<sup>2</sup> · Banchob Wann<sup>3</sup>

Received: 24 February 2020 / Accepted: 22 June 2020 / Published online: 30 June 2020  
© Springer-Verlag GmbH Germany, part of Springer Nature 2020

## Abstract

Due to the large surface area and unique electronic property, single-wall carbon nanotube (SWCNT) is being used for adsorption and detection nanomaterials, which can be used to reduce the CO pollution effect on the environment. In the present work, the adsorptions of single and multiple CO molecules on pristine and transition metal (TM = Fe-, Ru-, and Os)-doped SWCNT were investigated in terms of geometric, energetic, and electronic properties using density functional theory calculation. Calculated results display that the adsorption of CO molecule on the SWCNTs is energetically favorable. The TM-doped SWCNT are more highly interactive to CO adsorption than that of pristine SWCNT. An Os-doped SWCNT displays the strongest interaction with single and multiple CO molecules comparing with the Fe- and Ru-doped SWCNT. The TM doping on SWCNT can induce the charge transfer between CO molecule and the SWCNT. The energy gap and density of state are clearly changed when CO molecule interacts with TM-doped SWCNT, resulting in dramatic changes of their electronic properties. Therefore, TM-doped SWCNT are possibly used as potential CO storages/absorbents or sensor material for CO detection in the environment.

**Keywords** Adsorption · Carbon monoxide · Carbon nanotube · Density functional theory · Transition metal doping

## Introduction

Single-walled carbon nanotubes (SWCNT) are novel material which considerably interests in many scientific areas due to their excellent electronic, mechanical, physical, and chemical

properties toward the development of potential technological applications, such as molecular adsorption and sensor [1–4]. Under molecular adsorption, SWCNT can change their electronic property by charge transfer processes, resulting in high electronic sensitivity [5]. Thus, SWCNT-based materials serve as chemical sensors. Small gas interaction with nanostructure surfaces is a subfield of great interest due to potential applications such as gas storage and sensor [5–7]. Phenomenon of specific adsorption of small gas on nanostructure surfaces has been the subject of a number of theoretical papers. Most of them focus on the interaction of small gas with SWCNT [8–10]. However, the pristine SWCNT has been demonstrated to be sensor for detecting small gas molecules with long response time, low sensitivity, and low selectivity. Thus, the improvement of response time, sensitivity, and selectivity including to stability of pristine SWCNT for gas detection is intensively considered [11, 12]. To overcome the insensitivity of pristine SWCNT to gas, many modification schemes have been proposed [13–16]. In particular, the decorating of impurity atoms into SWCNT represents significant improvements for gas detection [17–19].

**Electronic supplementary material** The online version of this article (<https://doi.org/10.1007/s00894-020-04457-7>) contains supplementary material, which is available to authorized users.

✉ Banchob Wann  
banchobw@gmail.com

- <sup>1</sup> Computational Chemistry Center for Nanotechnology and Department of Chemistry, Faculty of Science and Technology, Rajabhat Maha Sarakham University, Maha Sarakham 44000, Thailand
- <sup>2</sup> Department of Chemistry, Faculty of Science, Buriram Rajabhat University, Buriram 31000, Thailand
- <sup>3</sup> Department of Chemistry, Center of Excellence for Innovation in Chemistry and Supramolecular Chemistry Research Unit, Faculty of Science, Mahasarakham University, Maha Sarakham 44150, Thailand

There are many literature about the SWCNT sensors as a detector for many gases such as NO [17, 18], SO<sub>2</sub> [20], O<sub>2</sub> [21], NH<sub>3</sub> [22], NO<sub>2</sub> [22, 23], CO<sub>2</sub> [23], H<sub>2</sub>CO [24], H<sub>2</sub>S [25], HCN [26], and C<sub>2</sub>H<sub>2</sub> [26] including to CO molecule [14, 17–19]; and the change in electronic property of SWCNTs occurs during gas adsorption process. Carbon monoxide is one of the most dangerous gases in air pollution. It is greatly toxic and tremendously dangerous because it is colorless and odorless [27]. Human beings cannot have timely alertness to its attendance. Consequently, an effective way to sense and remove CO molecule is needed, and the gas sensors with high selectivity and sensitivity to CO are highly desired. Theoretical investigations based on the density functional theory (DFT) have shown the outstanding adsorption ability and selectivity of Fe-doped graphene for CO molecule [28]. Graphenes doping with group 8B transition metals are more highly sensitive to CO adsorption than that of pristine graphene [29]. The Pd doping significantly improves interaction strength between CO molecules and the graphene [30]. Traditionally, B-doped C<sub>3</sub>N monolayer is among the most potential catalysts for oxidation of CO [31]. Recently, many reports suggest that impurity atom-doped SWCNT can be used as a highly sensitive CO sensor [32–34]. The adsorption of CO molecule on Al-doped SWCNT was studied through DFT computation by Wang and co-workers [32]. The Al-doped SWCNT shows high sensitivity to CO comparing with the pristine SWCNT. The DFT calculations reveal that the electrical conductivity of Fe-doped SWCNT is changed due to CO adsorption. These findings suggest that the Fe-doped SWCNT has sensitivities to CO molecules [33]. Theoretical calculation plays an important role of metal doping to improve the sensitivity and stability of SWCNT for gas adsorption and detection [34].

In the present study, an attempt has been made to scrutinize the properties of single and multiple CO molecule adsorptions onto Fe-, Ru-, and O-doped SWCNT using DFT calculation. A DFT investigation has been performed for CO molecule adsorption on pristine SWCNT and improvement of the weak ability of pristine SWCNT to adsorb CO molecule up to three molecules using Fe-, Ru-, and Os-doped SWCNT. Moreover, the TM-SWCNT which shows the strongest adsorption ability to CO molecule will be selected for further study the adsorption of CO up to five molecules. The structural stability, as well as electronic properties and interaction behaviors of CO molecules on pristine and Fe-, Ru-, and Os-doped SWCNT, will be explored.

## Computational details

An armchair (5,5) single-walled carbon nanotube containing 70 carbon and 20 hydrogen atoms was considered. For doping structures, one of the carbon atoms (defined as C1) in the 4th

layer of SWCNT was substituted by Fe, Ru, or Os atom, whereas the C atoms around the modified atom were defined as follows: C2, C3, and C4. The single and multiple CO molecules adsorbed on pristine, Fe-, Ru-, and Os-doped SWCNT by C or O atom of CO down to tube were chosen for the adsorption study. In the first configuration, CO interacts with SWCNT via its C atom down to tube (C<sub>CO</sub>/SWCNT) while in the second configuration CO interacts with SWCNT via its O atom down to tube (O<sub>CO</sub>/SWCNT). All structures were calculated by GAUSSIAN 09 software [35] and carried out using the intensive DFT method at the B3LYP/LanL2DZ theoretical level [36–41]. The B3LYP is an intensive and favorite functional in condensed matter which has been shown to perform adequately well for nanostructures [14, 17, 20, 22, 23, 26, 29, 42–44]. The highest occupied molecular orbital energies ( $E_{\text{HOMO}}$ ), the lowest unoccupied molecular orbital energies ( $E_{\text{LUMO}}$ ), and the energy gaps ( $E_{\text{gap}}$ ) referred to the energy difference between HOMO and LUMO orbitals were investigated. The partial charge transfers (PCTs) during CO adsorption were defined as a change in charges of CO during the adsorption process by means of the natural bond orbital (NBO) analysis implemented in GAUSSIAN 09 software. The electronic density of states (DOSs) of all systems was calculated and plotted by using the GaussSum 2.1.4 program [45]. The molecular graphics of all optimized structures were generated with the MOLEKEL 4.3 program [46].

The adsorption energies ( $E_{\text{ads}}$ ) of single and multiple CO molecules adsorbed on pristine and TM-doped SWCNT were obtained from Eqs. (1) to (2), respectively.

$$E_{\text{ads}} = E_{\text{CO/SWCNT}} - E_{\text{SWCNT}} - E_{\text{CO}} \quad (1)$$

$$E_{\text{ads}} = E_{n\text{CO/SWCNT}} - E_{(n-1)\text{CO/SWCNT}} - E_{\text{CO}} \quad (2)$$

where  $E_{\text{CO/SWCNT}}$  was the total energies of single CO adsorbed on pristine or TM-doped SWCNT.  $E_{n\text{CO/SWCNT}}$  and  $E_{(n-1)\text{CO/SWCNT}}$  were the total energies of  $n\text{CO}$  ( $n = 2-5$ ) adsorbed on pristine or TM-doped SWCNT, whereas  $E_{\text{SWCNT}}$  was the total energies of the pristine or TM-doped SWCNT, and  $E_{\text{CO}}$  was the total energies of isolated CO. By this explanation,  $\Delta E_{\text{ads}} < 0$  corresponds to exothermic process, which leads to a stable structure.

## Results and discussion

### Geometrical structures of pristine and TM-doped SWCNT and their adsorptions with CO

Firstly, the geometrical structures of pristine and TM-doped SWCNT and their CO adsorptions with single and multiple

CO molecules were calculated and analyzed. The optimized structures of pristine, Fe-, Ru-, and Os-doped SWCNT are shown in Fig. S1 of Supplementary material. The selected B3LYP/LanL2DZ geometrical parameters of single and multiple CO molecules adsorbed on pristine, Fe-, Ru-, and Os-doped SWCNT by pointing its C and O atoms down to tube are listed in Tables 1 and 2. The C1 atom in the pristine SWCNT and the C (C2, C3, and C4) atoms around the C1 or TM atom in the pristine or TM-SWCNT were selected to be active sites for CO adsorption on the SWCNT. The calculated results show that the C1–C2, C1–C3, and C1–C4 bond lengths of pristine SWCNT are approximately 1.442, 1.418, and 1.442 Å, respectively. The calculated C2–C1–C3, C3–C1–C4, and C4–C1–C2 bond angles of pristine SWCNT are estimated to be 118.6, 118.6, and 120.3°, respectively. The computed energy gap of pristine SWCNT is found to be 2.014 eV. Taking into account, the average C–C bond lengths and energy gap of pristine SWCNT obtained from the B3LYP/LanL2DZ theoretical level are found in good agreement with the C–C bond lengths ( $1.4 \pm 0.02$  Å) and energy gap (2.5 eV) obtained from the previous experimental reports [47]. Then, the B3LYP/LanL2DZ theoretical level was suitable for the present work.

After replacing C1 atom with the TM, the geometrical structure of the pristine SWCNT is significantly distorted because the TM–C bond lengths are longer than C–C bond lengths and C–TM–C bond angles are narrower than C–C–C bond angles. It has been previously shown that there is a worthy agreement between the results of this technique [19, 23, 28]. Among the TM-SWCNTs, a TM impurity atom is protruded out of the tube surface to decrease stress owing to its larger size compared with C atom. The B3LYP/LanL2DZ-optimized structures of single and multiple molecules of CO adsorbed on pristine SWCNT are shown in Figs. 1, 2, and 3. It is clearly seen that the geometrical structure of pristine SWCNT is slightly changed after CO adsorptions. The adsorption distances between the adsorption site and the nearest atom of the CO molecule and the C–O bond length of the adsorbed CO molecule for all the stability systems were also analyzed. The calculated results show that the adsorption distances between the pristine SWCNT surface and a CO molecule when pointing its C and O atoms toward the tube are calculated to be 3.447 and 3.305 Å, respectively, whereas the adsorption distances between multiple CO molecules and the pristine SWCNT are in the range 3.452–3.591 Å. The large adsorption distance values indicate that pristine SWCNT undergoes the weak interaction with CO molecule. In addition, the C–O bond lengths of CO molecule adsorbed on pristine SWCNT are 1.166 and 1.165 Å, when pointing its C and O atoms to the tube, respectively. This means that after CO adsorptions, the C–O bond length of free CO molecule (1.166 Å) is slightly changed, demonstrating that the CO molecule is not dissociated through the adsorption process, which

gives good matches with the theoretical values of 1.138 Å [48] and with the experimental value of 1.128 Å [49].

The optimized structures of single and multiple CO molecules adsorbed on the Fe-, Ru-, and Os-doped SWCNT are shown in Figs. 1, 2, and 3. The selected geometrical parameters of single and multiple CO molecules adsorbed on pristine, Fe-, Ru-, and Os-doped SWCNT are listed in Tables 1 and 2. The TM–C bond lengths of CO/TM-SWCNT at the adsorption site are longer than that of TM-SWCNT, while CO/TM-doped SWCNT, the C–TM–C bond angles of CO/TM-doped SWCNT, are narrow, compared with the system without CO adsorption. This means that the strong interaction between CO molecule and TM-SWCNT is formed. The adsorption distances between the TM atom-doped SWCNT and CO molecule are found in range of 1.848–1.998 (CO/TM-SWCNT), 2.006–2.346 (CO/TM-SWCNT), 1.822–1.996 (2CO/TM-SWCNT), 2.159–2.412 (2CO/TM-SWCNT), 1.811–2.004 (3CO/TM-SWCNT), and 2.188–2.443 Å (3CO/TM-SWCNT), much shorter than that of the pristine SWCNT. The result confirms the strong interaction between CO molecule and the TM-SWCNT. That means that there is a strong interaction formed between TM atom and C or O atom of CO molecule. This finding is in accordance with the previous reports [17, 19]. Zhang and Gong calculated the interior Fe–O distance to be 1.808 Å, by the CAM–B3LYP functional [17]. The adsorption distances of C atom down to tube are shorter than O atom down to the tube. This indicates that when C atom of CO molecule is close to the tube, their interactions with TM-doped SWCNT are stronger than that of O atom. This is similar to the CO adsorbed on the VIII B group-doped graphene nanosheet (GNS) [29] and Al-doped SWCNT [32]. The C–O bond lengths of CO molecule adsorbed on TM-doped SWCNT are found in the range between 1.174–1.182 and 1.164–1.173 Å, when C and O atoms are close to the tube, respectively, which slightly elongate (except for 2CO/Ru-SWCNT, 2CO/Fe-SWCNT, 3CO/Ru-SWCNT, and 3CO/Fe-SWCNT). Moreover, the C–O bond lengths of CO molecule adsorbed on TM-doped SWCNT are in actual fact similar to the C–O bond lengths which are reported, based on CO adsorption in previous theoretical investigation, such as Pd-doped SWCNT [19], Fe-doped GNS [29], VIII B group-doped GNS [29], and Al-doped GNS [50].

### Adsorption energies of CO adsorbed on pristine and TM-doped SWCNT

To determine the most stable adsorbed structures of single and multiple CO molecules adsorbed on the pristine, Fe-, Ru-, and Os-doped SWCNT, the adsorption energies ( $E_{\text{ads}}$ ) are computed and listed in Table 3. Considering the adsorption energies of single and multiple CO molecules adsorbed on pristine and TM-doped SWCNT, the obtained results show that the CO molecule is thermodynamically bound

**Table 1** The selected geometrical parameters of  $\underline{\text{CO}}$  adsorbed on pristine, Fe-, Ru-, and Os-doped SWCNT by pointing its C atom of  $\underline{\text{CO}}$  toward the SWCNT adsorption site

Species	Bond lengths <sup>a,b</sup>	Bond lengths (Å)	Bond angles <sup>a,b</sup>	Bond angles (°)	AD ranges (Å)	CO distances (Å)
$\underline{\text{CO}}$ /SWCNT	C1–C2	1.441	C2–C1–C3	118.7	C1–	C5–O = 1.166
	C1–C3	(1.442) <sup>c</sup>		(118.6) <sup>c</sup>		
	C1–C4	1.419 (1.418)		118.8 (118.6)		
$2\underline{\text{CO}}$ /SWCNT		1.441	C3–C1–C4	120.1	C5 = 3.447	
	C1–C2	1.441	C4–C1–C2	(120.3)		
	C1–C3	1.415	C2–C1–C3	118.8	C1–	C5–
	C1–C4	1.441	C3–C1–C4	118.8	C5 = 3.463	O1 = 1.166
$3\underline{\text{CO}}$ /SWCNT		1.441	C4–C1–C2	120.2	C3–C6 = 3.591	C6–O2 = 1.166
	C1–C2	1.442	C2–C1–C3	118.6	C1–	C5–
	C1–C3	1.418	C3–C1–C4	118.6	C5 = 3.589	O1 = 1.165
	C1–C4	1.441	C4–C1–C2	120.2	C1–	C5–
$\underline{\text{CO}}$ /Fe–SWCNT					C6 = 3.527	O2 = 1.165
					C1–	C5–
					C7 = 3.535	O3 = 1.165
	Fe–C2	1.814	C2–Fe–C3	91.9 (94.4)	Fe–	C5–O = 1.174
	Fe–C3	(1.797)	C3–Fe–C4	91.9 (94.4)	C5 = 1.848	
	Fe–C4	1.875	C4–Fe–C2	97.6 (95.9)		
		(1.885)				
	1.814					
	(1.797)					
$2\underline{\text{CO}}$ /Fe–SWCNT	Fe–C2	1.863	C2–Fe–C3	89.1	Fe–	C5–
	Fe–C3	1.933	C3–Fe–C4	88.3	C5 = 1.843	O1 = 1.175
	Fe–C4	1.875	C4–Fe–C2	92.1	Fe–	C6–
$3\underline{\text{CO}}$ /Fe–SWCNT					C6 = 1.822	O2 = 1.174
	Fe–C2	1.954	C2–Fe–C3	85.1	Fe–	C5–
	Fe–C3	1.983	C3–Fe–C4	85.1	C5 = 1.841	O1 = 1.173
	Fe–C4	1.954	C4–Fe–C2	89.3	Fe–	C6–
$\underline{\text{CO}}$ /Ru–SWCNT					C6 = 1.811	O2 = 1.173
					Fe–C7 = 1.842	C7–O3 = 1.173
					C5 = 1.998	C5–O = 1.177
	Ru–C2	1.930	C2–Ru–C3	89.1 (90.0)	Ru–	
	Ru–C3	(1.908)	C3–Ru–C4	89.5 (90.0)		
	Ru–C4	2.033 (1.939)				
		1.930	C4–Ru–C2	89.1 (95.3)		
	(1.908)					
$2\underline{\text{CO}}$ /Ru–SWCNT	Ru–C2	2.004	C2–Ru–C3	84.8	Ru–	C5–
	Ru–C3	2.069	C3–Ru–C4	85.0	C5 = 1.996	O1 = 1.177
	Ru–C4	1.976	C4–Ru–C2	88.9	Ru–	C6–
$3\underline{\text{CO}}$ /Ru–SWCNT					C6 = 1.986	O2 = 1.175
	Ru–C2	2.062	C2–Ru–C3	82.4	Ru–	C5–
	Ru–C3	2.101	C3–Ru–C4	82.4	C5 = 2.004	O1 = 1.174
	Ru–C4	2.062	C4–Ru–C2	86.2	Ru–	C6–
$\underline{\text{CO}}$ /Os–SWCNT					C6 = 1.982	O2 = 1.173
					Ru–	C7–
					C7 = 2.004	O3 = 1.174
	Os–C2	1.938	C2–Os–C3	87.6 (90.6)	Os–	C5–O = 1.182
	Os–C3	(1.911)	C3–Os–C4	87.6 (90.6)	C5 = 1.972	
	Os–C4	2.044	C4–Os–C2	94.9 (97.6)		
		(1.943)				
	1.938					
	(1.912)					
$2\underline{\text{CO}}$ /Os–SWCNT	Os–C2	2.025	C2–Os–C3	84.1	Os–	C5–
	Os–C3	2.085	C3–Os–C4	85.3	C5 = 1.962	O1 = 1.182
	Os–C4	1.981	C4–Os–C2	89.4	Os–	C6–
$3\underline{\text{CO}}$ /Os–SWCNT					C6 = 1.967	O2 = 1.179
	Os–C2	2.082	C2–Os–C3	82.0	Os–	C5–
	Os–C3	2.114	C3–Os–C4	82.0	C5 = 1.977	O1 = 1.177
	Os–C4	2.081	C4–Os–C2	85.8	Os–	C6–
CO molecule					C6 = 1.969	O2 = 1.176
					Os–	C7–
					C7 = 1.977	O3 = 1.177
C–O	1.166					

<sup>a</sup> C1, C2, C3, and C4 are atoms on the SWCNT which are defined in Fig. S1<sup>b</sup> Fe, Ru, or Os metal atom which is doped on SWCNT, see Fig. 1<sup>c</sup> In parentheses are selected bond angles of pristine and TM-doped SWCNT without CO adsorption in degree

**Table 2** The selected geometrical parameters of  $\underline{\text{CO}}$  adsorbed on pristine, Fe-, Ru-, and Os-doped SWCNT by pointing its O atom of  $\underline{\text{CO}}$  toward the SWCNT adsorption site

Species	Bond lengths <sup>a,b</sup>	Bond lengths (Å)	Bond angles <sup>a,b</sup>	Bond angles (°)	AD ranges (Å)	CO distances (Å)
$\underline{\text{CO}}$ /SWCNT	C1–C2	1.441	C2–C1–C3	118.6	C1–	C5–O = 1.165
	C1–C3	1.417	C3–C1–C4	118.6	O = 3.305	
	C1–C4	1.441	C4–C1–C2	120.2		
$2\underline{\text{CO}}$ /SWCNT	C1–C2	1.441	C2–C1–C3	118.6	C1–	C5–
	C1–C3	1.417	C3–C1–C4	118.6	O1 = 3.552	O1 = 1.165
	C1–C4	1.441	C4–C1–C2	120.2	C3–	C6–
$3\underline{\text{CO}}$ /SWCNT	C1–C2	1.441	C2–C1–C3	118.6	O2 = 3.452	O2 = 1.164
	C1–C3	1.417	C3–C1–C4	118.6	C–	C5–
	C1–C4	1.441	C4–C1–C2	120.2	C5 = 3.582	O1 = 1.165
$\underline{\text{CO}}$ /Fe–SWCNT	Fe–C2	1.799	C2–Fe–C3	93.1	C1–	C6–
	Fe–C3	1.818	C3–Fe–C4	93.1	O2 = 3.472	O2 = 1.165
	Fe–C4	1.799	C4–Fe–C2	98.9	C–	C7–
$2\underline{\text{CO}}$ /Fe–SWCNT	Fe–C2	1.807	C2–Fe–C3	92.1	C7 = 3.551	O3 = 1.165
	Fe–C3	1.835	C3–Fe–C4	92.0	Fe–O = 2.066	C5–O = 1.171
	Fe–C4	1.824	C4–Fe–C2	96.5		
$3\underline{\text{CO}}$ /Fe–SWCNT	Fe–C2	1.829	C2–Fe–C3	91.2	Fe–	C5–
	Fe–C3	1.847	C3–Fe–C4	91.2	O1 = 2.231	O1 = 1.166
	Fe–C4	1.829	C4–Fe–C2	95.5	Fe–O2 = 2.159	C6–
$\underline{\text{CO}}$ /Ru–SWCNT	Ru–C2	1.911	C2–Ru–C3	89.0	O2 = 1.166	O2 = 1.166
	Ru–C3	1.950	C3–Ru–C4	89.0	Fe–	C7–
	Ru–C4	1.911	C4–Ru–C2	95.1	O3 = 2.188	O3 = 1.165
$2\underline{\text{CO}}$ /Ru–SWCNT	Ru–C2	1.915	C2–Ru–C3	88.6	Ru–	C5–O = 1.670
	Ru–C3	1.959	C3–Ru–C4	88.3	O = 2.346	C5–
	Ru–C4	1.926	C4–Ru–C2	93.2	Ru–	C5–
$3\underline{\text{CO}}$ /Ru–SWCNT	Ru–C2	1.929	C2–Ru–C3	87.9	O1 = 2.369	O1 = 1.166
	Ru–C3	1.967	C3–Ru–C4	87.9	Ru–	C6–
	Ru–C4	1.929	C4–Ru–C2	92.2	O2 = 2.412	O2 = 1.166
$\underline{\text{CO}}$ /Os–SWCNT	Os–C2	1.915	C2–Os–C3	89.2	Ru–	C7–
	Os–C3	1.959	C3–Os–C4	89.2	O1 = 2.443	O1 = 1.164
	Os–C4	1.915	C4–Os–C2	97.0	Ru–	C6–
$2\underline{\text{CO}}$ /Os–SWCNT	Os–C2	1.924	C2–Os–C3	88.8	O2 = 2.442	O2 = 1.164
	Os–C3	1.969	C3–Os–C4	88.5	Ru–	C7–
	Os–C4	1.936	C4–Os–C2	94.0	O3 = 2.379	O3 = 1.165
$3\underline{\text{CO}}$ /Os–SWCNT	Os–C2	1.943	C2–Os–C3	87.8	O = 2.262	C5–O = 1.173
	Os–C3	1.980	C3–Os–C4	87.8	Os–	
	Os–C4	1.943	C4–Os–C2	92.2	O1 = 2.304	O1 = 1.171
$\underline{\text{CO}}$ /SWCNT					Os–	C6–
					O2 = 2.302	O2 = 1.170
					Os–	C5–
$2\underline{\text{CO}}$ /SWCNT					O1 = 2.322	O1 = 1.169
					Os–	C6–
					O2 = 2.322	O2 = 1.169
$3\underline{\text{CO}}$ /SWCNT					Os–	C7–
					O3 = 2.311	O3 = 1.169

<sup>a</sup> C1, C2, C3, and C4 are atoms on the SWCNT which are defined in Fig. S1<sup>b</sup> Fe, Ru, or Os metal atom which is doped on SWCNT, see Fig. S1

on the pristine and TM-doped SWCNT due to the negative values of  $E_{\text{ads}}$ . The adsorption energies of single and multiple CO molecules adsorbed on pristine SWCNT by pointing C and O atoms to the tube are  $-1.07$  ( $\underline{\text{CO}}$ /SWCNT),  $-0.41$  ( $\underline{\text{CO}}$ /SWCNT),  $-0.84$  ( $2\underline{\text{CO}}$ /SWCNT),

$-0.24$  ( $2\underline{\text{CO}}$ /SWCNT),  $-4.46$  ( $3\underline{\text{CO}}$ /SWCNT), and  $-2.50$  kcal/mol ( $3\underline{\text{CO}}$ /SWCNT). The small values of adsorption energy and charge transfer, and the large adsorption distance suggest that the adsorption ability of pristine SWCNT to CO molecule displays the weak interaction.

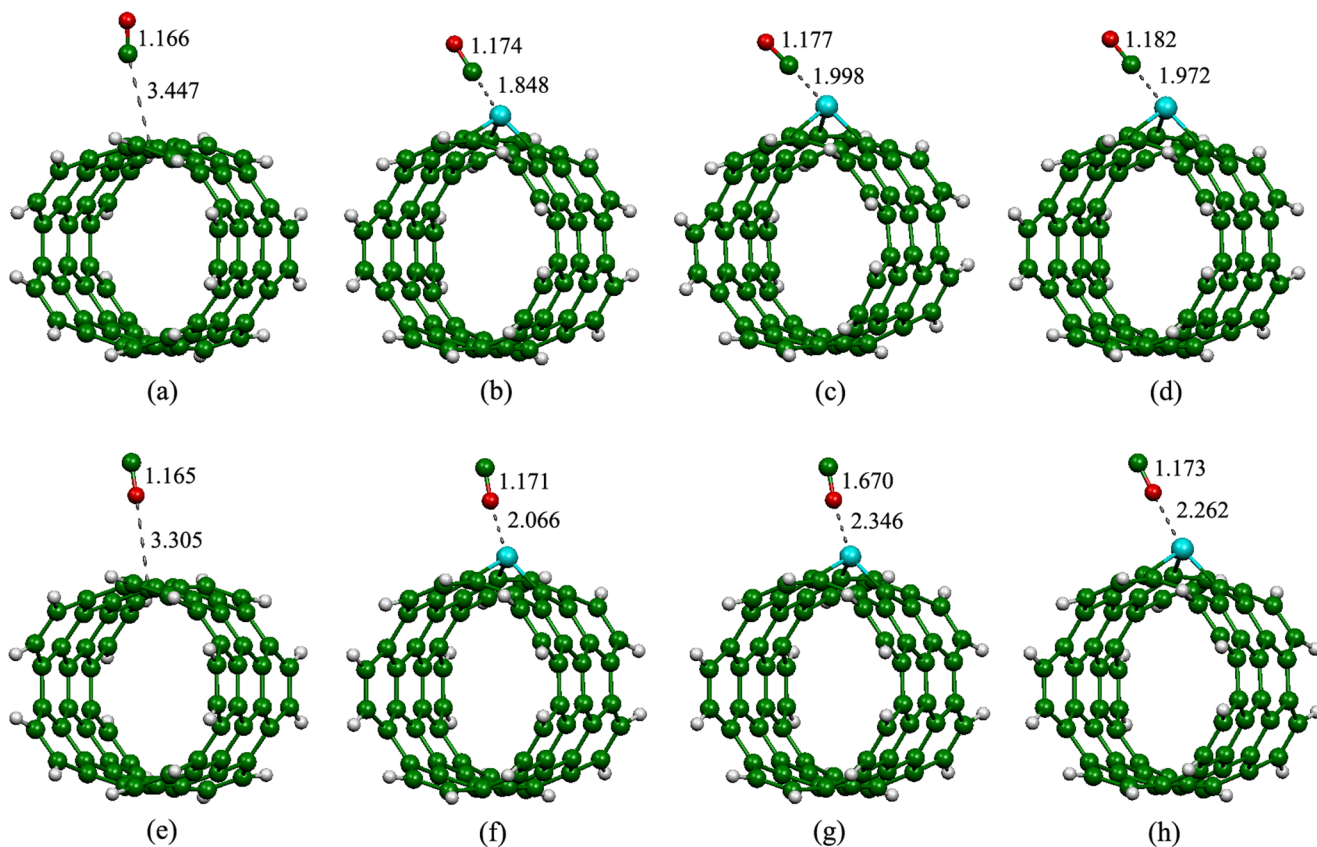


**Fig. 1** The B3LYP/LanL2DZ optimized structures of (a)  $\underline{\text{CO}}/\text{SWCNT}$ , (b)  $\underline{\text{CO}}/\text{Fe-SWCNT}$ , (c)  $\underline{\text{CO}}/\text{Ru-SWCNT}$ , (d)  $\underline{\text{CO}}/\text{Os-SWCNT}$ , (e)  $\underline{\text{CO}}/\text{SWCNT}$ , (f)  $\underline{\text{CO}}/\text{Fe-SWCNT}$ , (g)  $\underline{\text{CO}}/\text{Ru-SWCNT}$ , and (h)  $\underline{\text{CO}}/\text{Os-SWCNT}$ . Bond distances are in Å

This indicates that pristine SWCNT is slightly sensitive to CO molecule. The adsorption energies of single CO molecule adsorbed on TM-doped SWCNT by pointing C and O atoms to the tube are in the range between  $-42.78$  and  $-8.89$  kcal/mol. The adsorption abilities are found to be in the following order:  $\underline{\text{CO}}/\text{Os-SWCNT}$  ( $-42.78$  kcal/mol)  $>$   $\underline{\text{CO}}/\text{Fe-SWCNT}$  ( $-34.25$  kcal/mol)  $\approx$   $\underline{\text{CO}}/\text{Ru-SWCNT}$  ( $-31.57$  kcal/mol)  $\gg$   $\underline{\text{CO}}/\text{Fe-SWCNT}$  ( $-12.26$  kcal/mol)  $\approx$   $\underline{\text{CO}}/\text{Os-SWCNT}$  ( $-11.32$  kcal/mol)  $\approx$   $\underline{\text{CO}}/\text{Ru-SWCNT}$  ( $-8.89$  kcal/mol). The adsorption energies of two CO molecules adsorbed on TM-doped SWCNT by pointing C and O atoms to the tube are in the range between  $-42.78$  and  $-5.47$  kcal/mol. The adsorption abilities are found in the following order:  $2\underline{\text{CO}}/\text{Os-SWCNT}$  ( $-42.78$  kcal/mol)  $>$   $2\underline{\text{CO}}/\text{Fe-SWCNT}$  ( $-29.63$  kcal/mol)  $\approx$   $2\underline{\text{CO}}/\text{Ru-SWCNT}$  ( $-29.25$  kcal/mol)  $\gg$   $2\underline{\text{CO}}/\text{Os-SWCNT}$  ( $-7.53$  kcal/mol)  $\approx$   $2\underline{\text{CO}}/\text{Ru-SWCNT}$  ( $-6.42$  kcal/mol)  $\approx$   $2\underline{\text{CO}}/\text{Fe-SWCNT}$  ( $-5.47$  kcal/mol). The adsorption energies of three molecules of CO adsorbed on TM-doped SWCNT by pointing C and O atoms to the tube are in the range between  $-36.69$  and  $-4.53$  kcal/mol. The adsorption abilities are found in the following order:  $3\underline{\text{CO}}/\text{Os-SWCNT}$  ( $-36.69$  kcal/mol)  $>$   $3\underline{\text{CO}}/\text{Ru-SWCNT}$  ( $-24.83$  kcal/mol)  $\approx$   $3\underline{\text{CO}}/\text{Fe-SWCNT}$  ( $-23.42$  kcal/mol)  $\gg$   $3\underline{\text{CO}}/\text{Os-SWCNT}$  ( $-7.95$  kcal/mol)

$\approx 3\underline{\text{CO}}/\text{Ru-SWCNT}$  ( $-6.22$  kcal/mol)  $\approx 3\underline{\text{CO}}/\text{Fe-SWCNT}$  ( $-4.53$  kcal/mol). Thus, the adsorption distances between CO molecule and TM-SWCNT are shorter than those of pristine SWCNT, which lead to the higher adsorption energies of TM-SWCNT to CO molecule. The results indicate that the adsorption ability of SWCNT onto CO molecule is improved by TM doping, similar to the previous report of CO adsorbed on Fe- and Ni-doped SWCNT [17]. Previous DFT calculations indicated that the adsorption abilities of Pd-doped SWCNT [19], VIII-B-doped GNS [29], Al-doped SWCNT [32], and Fe-doped GNS [33] to CO molecule are also improved by impurity atom doping. The large values of adsorption energy and charge transfer and small adsorption distance suggest that CO molecule undergoes a strong interaction with TM-doped SWCNT. Comparing adsorption configurations with CO adsorption ability of TM-doped SWCNT by pointing C and O atoms of CO molecule to the adsorption sites, it is found that pointing C atom of CO molecule to the adsorption site shows higher adsorption ability than pointing O atom. The literature review indicates that adsorption via pointing C ( $\underline{\text{CO}}$ ) leads to a stronger interaction than that of pointing O ( $\underline{\text{CO}}$ ) [51]. For the adsorptions of single and multiple CO molecules on the TM-doped SWCNT, the Os-doped SWCNT displays the highest

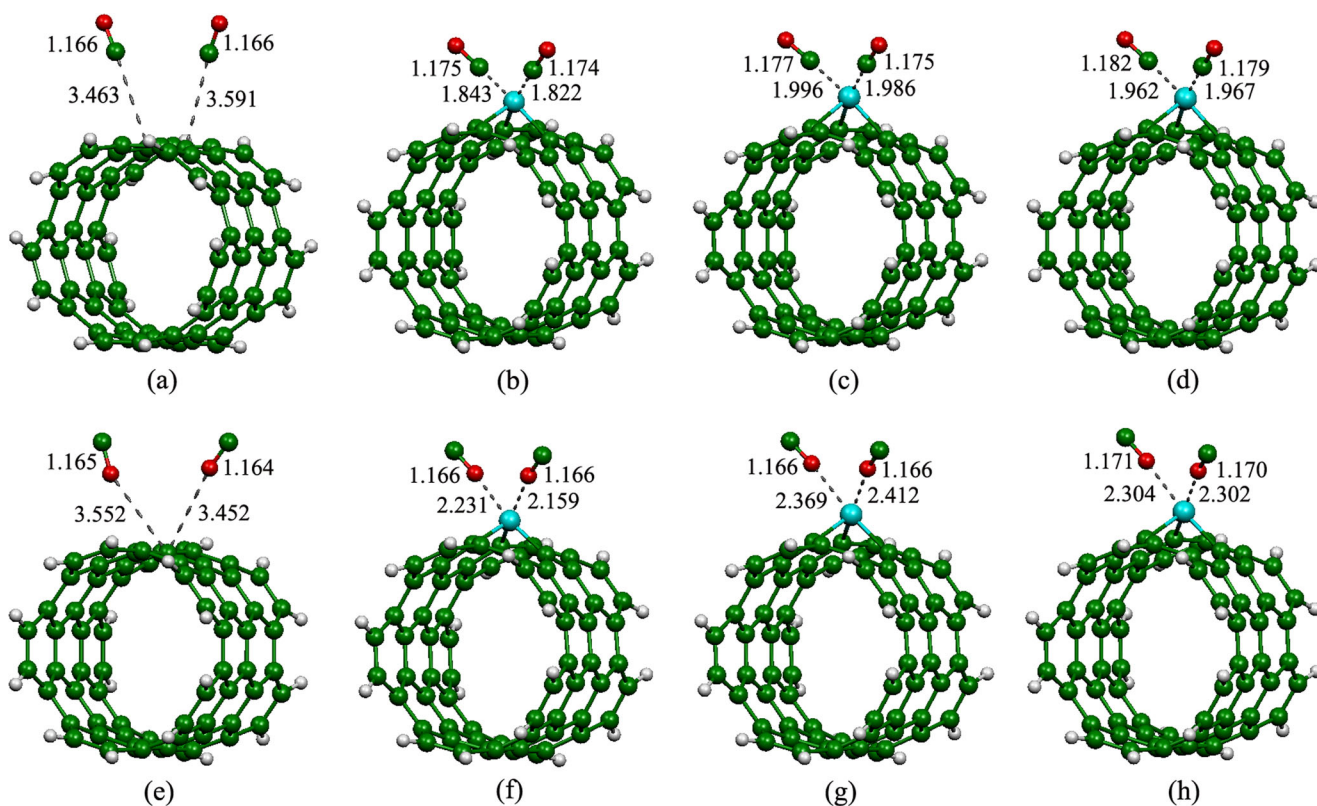


**Fig. 2** The B3LYP/LanL2DZ optimized structures of (a)  $2\text{CO}/\text{SWCNT}$ , (b)  $2\text{CO}/\text{Fe-SWCNT}$ , (c)  $2\text{CO}/\text{Ru-SWCNT}$ , (d)  $2\text{CO}/\text{Os-SWCNT}$ , (e)  $2\text{CO}/\text{SWCNT}$ , (f)  $2\text{CO}/\text{Fe-SWCNT}$ , (g)  $2\text{CO}/\text{Ru-SWCNT}$ , and (h)  $2\text{CO}/\text{Os-SWCNT}$ . Bond distances are in Å

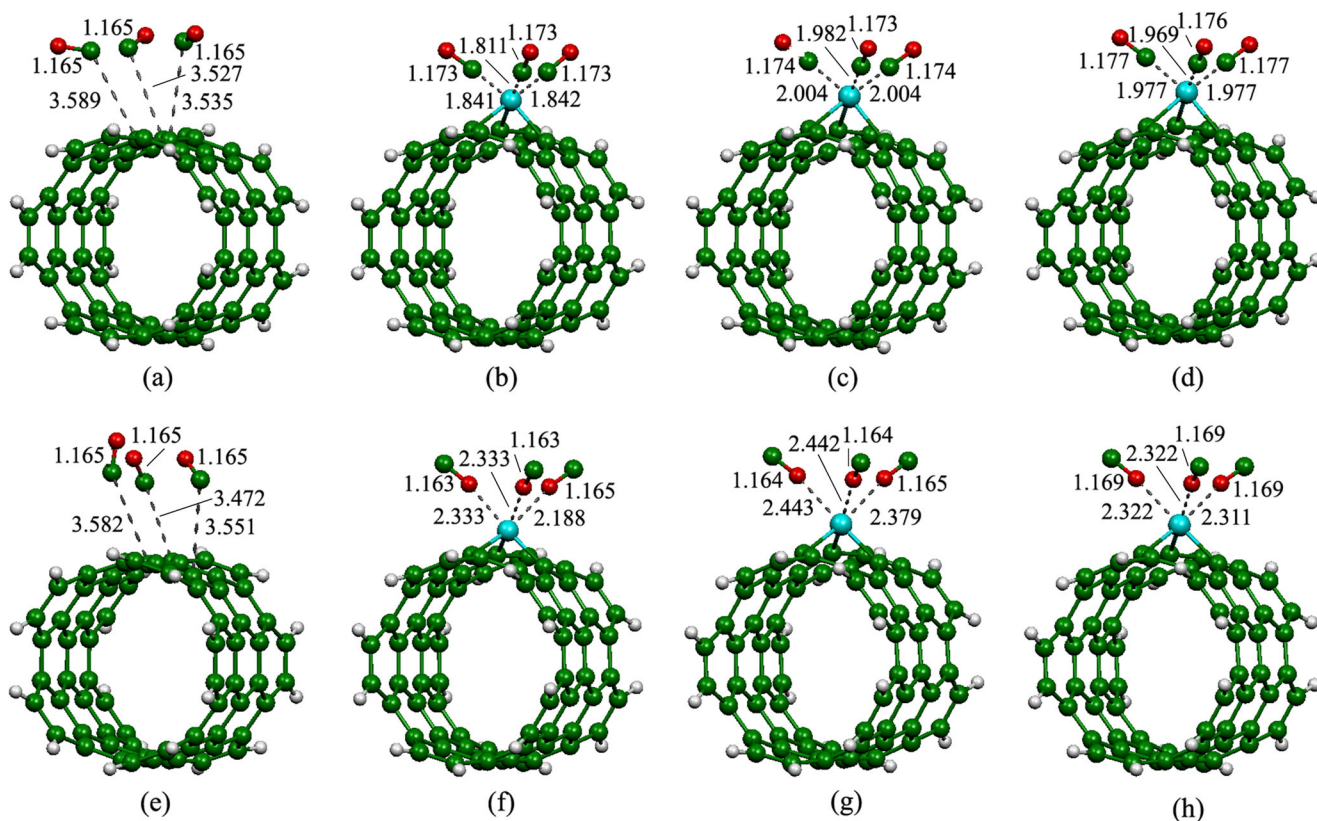


**Fig. 3** The B3LYP/LanL2DZ optimized structures of (a)  $3\text{CO}/\text{SWCNT}$ , (b)  $3\text{CO}/\text{Fe-SWCNT}$ , (c)  $3\text{CO}/\text{Ru-SWCNT}$ , (d)  $3\text{CO}/\text{Os-SWCNT}$ , (e)  $3\text{CO}/\text{SWCNT}$ , (f)  $3\text{CO}/\text{Fe-SWCNT}$ , (g)  $3\text{CO}/\text{Ru-SWCNT}$ , and (h)  $3\text{CO}/\text{Os-SWCNT}$ . Bond distances are in Å

**Table 3** Adsorption energies ( $E_{\text{ads}}$ , in kcal/mol), energy gap ( $E_{\text{gap}}$ , in eV), and partial charge transfers (PCT, in e) of CO adsorbed on the pristine and TM-doped SWCNTs

Reaction	$E_{\text{ads}}$	$E_{\text{HOMO}}$	$E_{\text{LUMO}}$	$E_{\text{gap}}$	$\Delta E_{\text{gap}}^a$	PCT
<u>CO</u> /SWCNT	-1.07	-4.871	-2.640	2.231	0.217	0.001
<u>2CO</u> /SWCNT	-0.84	-4.871	-2.640	2.231	0.217	0.001
<u>3CO</u> /SWCNT	-4.46	-4.898	-2.694	2.204	0.190	0.007
<u>CO</u> /Fe-SWCNT	-34.25	-4.708	-3.266	1.442	0.177	0.120
<u>2CO</u> /Fe-SWCNT	-29.63	-4.789	-3.374	1.415	0.204	0.117
<u>3CO</u> /Fe-SWCNT	-23.42	-4.816	-3.646	1.170	0.449	0.565
<u>CO</u> /Ru-SWCNT	-31.57	-4.708	-3.266	1.442	0.218	0.082
<u>2CO</u> /Ru-SWCNT	-29.25	-4.789	-3.428	1.361	0.299	0.231
<u>3CO</u> /Ru-SWCNT	-24.83	-4.789	-3.592	1.197	0.463	0.479
<u>CO</u> /Os-SWCNT	-43.81	-4.708	-3.374	1.333	0.245	0.025
<u>2CO</u> /Os-SWCNT	-42.78	-4.817	-3.511	1.306	0.272	0.135
<u>3CO</u> /Os-SWCNT	-36.69	-4.817	-3.647	1.170	0.408	0.398
<u>CO</u> /SWCNT	-0.41	-4.871	-2.640	2.231	0.127	0.002
<u>2CO</u> /SWCNT	-0.24	-4.844	-2.640	2.204	0.100	0.006
<u>3CO</u> /SWCNT	-2.50	-4.871	-2.667	2.204	0.100	0.004
<u>CO</u> /Fe-SWCNT	-12.26	-4.626	-2.993	1.633	0.014	0.042
<u>2CO</u> /Fe-SWCNT	-5.47	-4.599	-2.885	1.714	0.095	0.097
<u>3CO</u> /Fe-SWCNT	-4.53	-4.572	-2.830	1.710	0.449	0.052
<u>CO</u> /Ru-SWCNT	-8.89	-4.572	-2.858	1.714	0.054	0.038
<u>2CO</u> /Ru-SWCNT	-6.42	-4.544	-2.830	1.714	0.054	0.062
<u>3CO</u> /Ru-SWCNT	-6.22	-4.544	-2.803	1.741	0.081	0.108
<u>CO</u> /Os-SWCNT	-11.32	-4.599	-3.075	1.524	0.054	0.008
<u>2CO</u> /Os-SWCNT	-7.53	-4.544	-2.884	1.660	0.082	0.021
<u>3CO</u> /Os-SWCNT	-7.95	-4.517	-2.857	1.660	0.082	0.052

<sup>a</sup>  $\Delta E_{\text{gap}}$  is defined as the difference between  $E_{\text{gap}}$  of bare SWCNT and  $E_{\text{gap}}$  of CO adsorbed on SWCNT

interaction with single CO molecule in comparison with the other species, Fe- and Ru-doped SWCNT. Base on the Pearson hard-soft acid-base (HSAB) concept, Fe is borderline atom whereas Ru and Os are soft atoms, in which C is soft atom whereas O is hard atom. Then TM atoms are more favorite C atom than that of O atom [52].

Due to the Os-SWCNT showing the strongest adsorption strength compared with Fe- and Ru-SWCNT (except for CO/Fe-SWCNT), therefore, Os-SWCNT was selected to study the adsorption abilities of four and five CO molecules. The optimized structures of four and five CO molecules adsorbed on Os-SWCNT are displayed in Fig. S2. From this figure, it is clearly seen that the highest storage number in the first adsorption layer of the Os-doped SWCNT to CO molecules is three CO molecules. Besides, it is found that the CO up to four and five molecules can be adsorbed on an Os-doped SWCNT in which the adsorption energies are -2.40 (4CO/Os-SWCNT), -1.34, (4CO/Os-SWCNT), -2.53 (5CO/Os-SWCNT), and -2.03 kcal/mol (5CO/Os-SWCNT).

## Electronic properties for the CO adsorbed on pristine and TM-doped SWCNT

In order to clearly present the charge transfer induced by adsorption of CO molecules, the partial charge transfers (PCTs) between CO and pristine and TM-doped SWCNT were calculated from the natural bond orbital charge (NBO) analysis (see Table 3). This may be understood by the fact that the CO adsorption tend to change the hybridization of atoms at binding site from  $sp^2$  to  $sp^3$ -like hybridization. The PCTs were defined as  $Q_{\text{CO/SWCNT}} - Q_{\text{free CO}}$ , where  $Q_{\text{CO/SWCNT}}$  was the total charge of CO adsorbed on pristine and TM-doped SWCNT, and  $Q_{\text{free CO}}$  was the total charge of CO in free case. A positive value of PCT means the electron transfer from CO molecule to tube. In contrast, a negative value means the electron transfer from tube to CO molecule. Considering the PCTs of single and multiple CO molecules adsorbed on pristine and TM-doped SWCNT, it is found that small charges are transferred from CO molecule to the pristine SWCNT (0.001–0.007 e). In the other hand, large charges are transferred from CO molecule to the TM-doped SWCNT (0.008 to 0.565 e), possibly due to that a part of electrons gain for TM atom after CO adsorption. This indicates that the TM doping influences the electronic properties of SWCNT, which is in well agreement with the result of electron transfer of CO interaction with Pd-doped SWCNT [19] and Al-doped SWCNT [32].

The chemical activities of the SWCNT to CO molecule can be investigated by the HOMO–LUMO energy gap ( $E_{\text{gap}}$ ) that is a significant parameter relying on the HOMO and LUMO energy levels (see Table 3). The calculated energy gaps for pristine, Fe-, Ru-, and Os-doped SWCNT are 2.014, 1.619, 1.660, and 1.578 eV, respectively. The chemical stability of pristine SWCNT will be decreased due to TM doping, and thus, chemical activity of such system will be significantly increased. When a single and multiple CO molecules adsorbed on the Fe-, Ru-, and Os-doped SWCNT in stable configurations, the changes of their energy gaps are found in the range of 0.86–15.52%. For three CO molecules, the  $E_{\text{gap}}$  of Ru-SWCNT displays the highest change at 27.89% after CO adsorption by C atom pointing to tube. The same behavior concerning the change of the energy gap after the CO adsorption is also observed for VIII B group-doped GNS [29], Fe-doped GNS [33], and N/B-doped GNS [53].

For examining the sensitivity of TM-doped SWCNT to the CO molecules, two indexes, work function ( $\Phi$ ), and  $E_{\text{g}}$  are calculated. The  $E_{\text{g}}$  is an electronic parameter to quantify a semiconductor sensitivity toward chemical agent. Then, the electric conductance ( $\sigma$ ) was calculated using the following formula:

$$\sigma = AT^{3/2} \exp(-E_{\text{g}}/2kT) \quad (3)$$



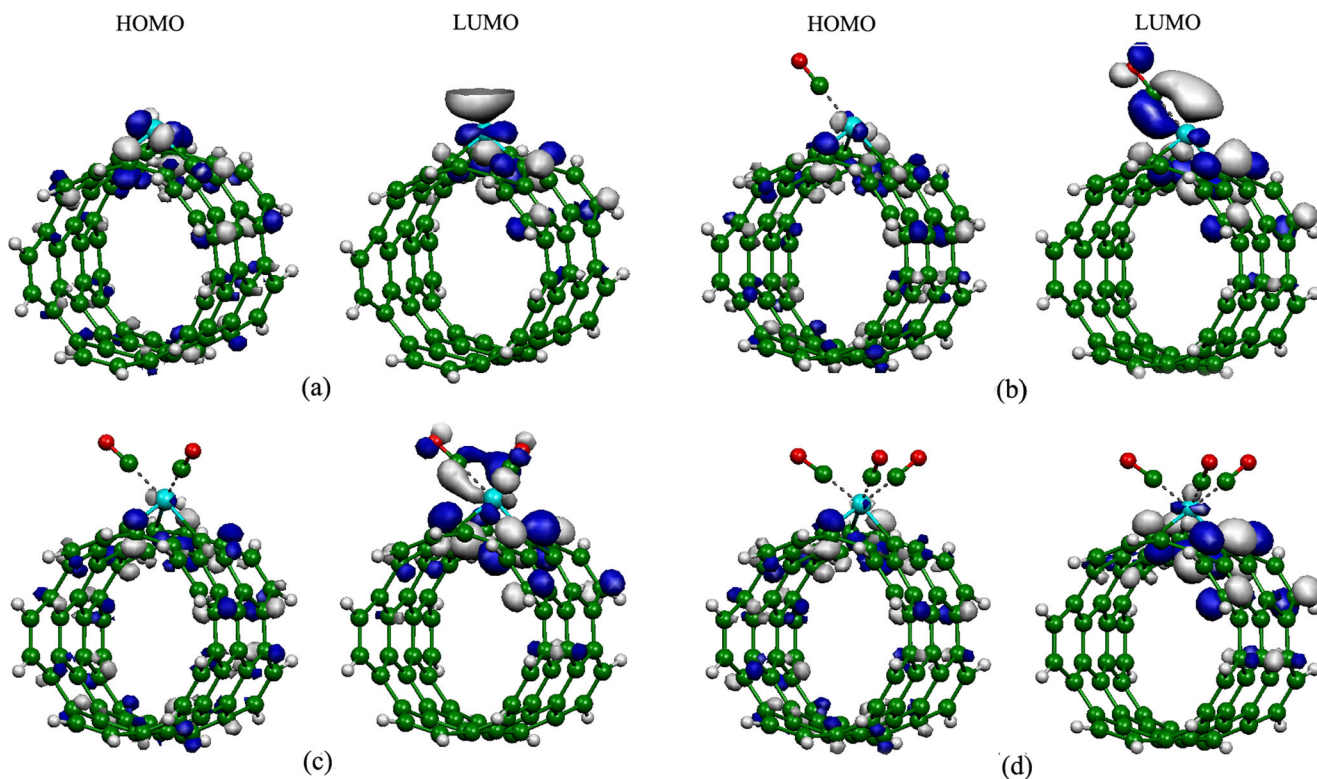


**Fig. 4** Typical contour plots of the HOMO and LUMO of (a) Os-SWCNT, (b)  $\underline{\text{CO}}$ /Os-SWCNT, (c)  $\underline{2\text{CO}}$ /Os-SWCNT, and (d)  $\underline{3\text{CO}}$ /Os-SWCNT

where  $A$  is a constant in dimension of electrons/m<sup>3</sup>K<sup>3/2</sup>,  $k$  is the Boltzmann's constant, and  $T$  the temperature [54]. An above equation implies that a decrease in the gap exponentially enhances the  $\sigma$  of adsorbent, linking to the chemical agent existence. Also, the impact of gas adsorption on the work function and Fermi level of the sensor is examined. If the adsorption of gas molecules increases or decreases the work function of sensor, it will produce an electrical signal [55]. The work function is also affected by TM doping. It is defined as:

$$\Phi = E_{\text{vac}} - E_{\text{F}} \quad (4)$$

where  $E_{\text{vac}}$  is the reference vacuum energy calculated from the electrostatic potential in the vacuum energy. The Fermi level energy is computed as follows:  $E_{\text{F}} = E_{\text{HOMO}} + (E_{\text{LUMO}} - E_{\text{HOMO}})/2$ . The calculated results show that the work function values of CO adsorption on pristine, Fe-, Ru-, and Os-doped SWCNT are 3.76 ( $\Phi$  of pristine SWCNT = 3.76 eV), 3.99 ( $\Phi$  of Fe-SWCNT = 3.88 eV), 3.99 ( $\Phi$  of Ru-SWCNT = 3.80 eV), and 4.04 eV ( $\Phi$  of Os-SWCNT = 3.81 eV), respectively. Thus, the electron emission from the surface of tube will alter after by CO adsorption. It shows that the TM-doped SWCNT could be a plausible  $\Phi$ -type CO gas sensor.

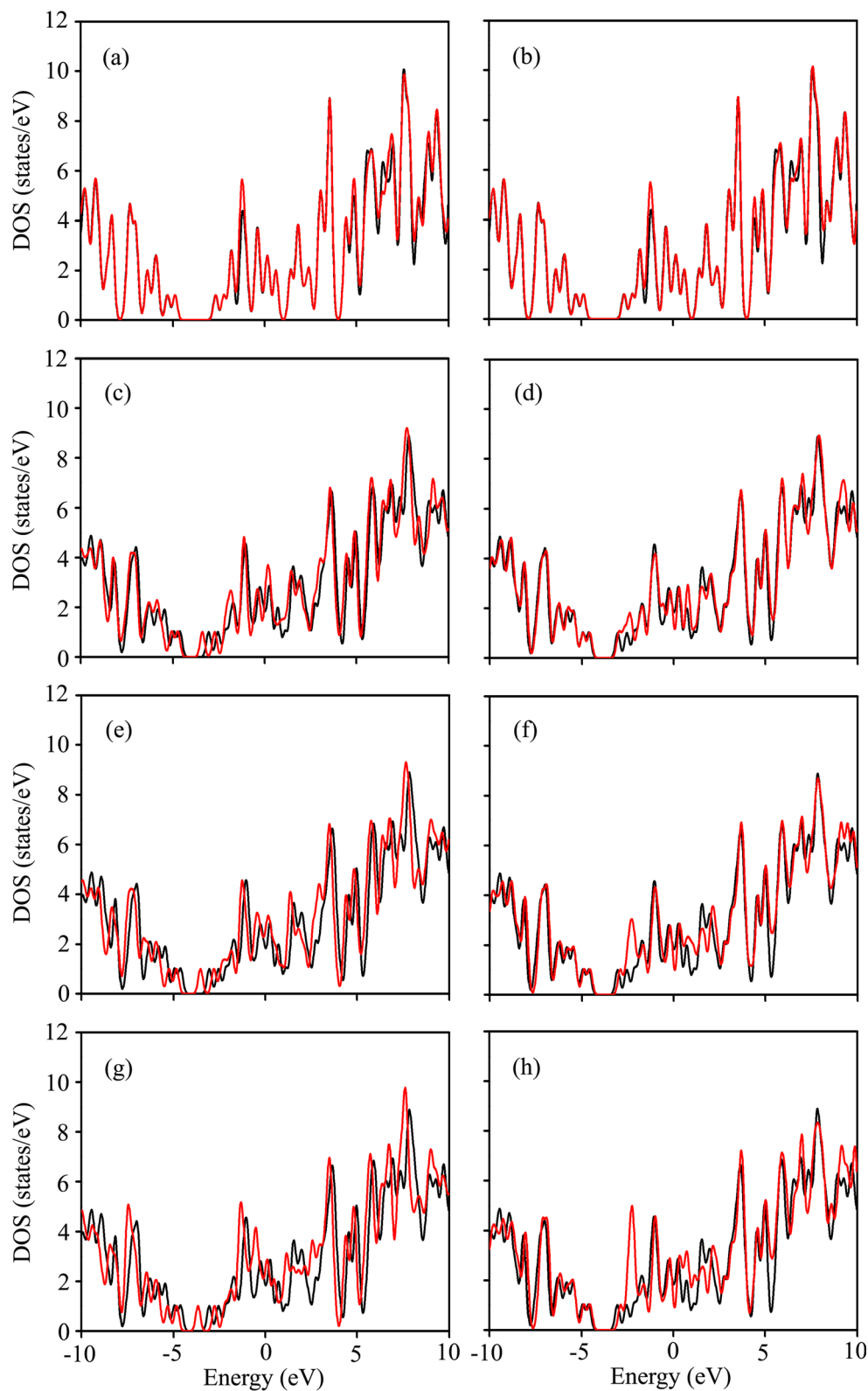
Furthermore, the effect of adsorption behavior of the single and multiple CO molecules on the pristine and TM-doped SWCNT on orbital distributions was investigated. The frontier molecular orbital distributions or HOMO and

LUMO plots of pristine, Fe-, Ru-, and Os-doped SWCNT (Fig. S1) and their CO adsorptions as configurations of CO molecule when pointing C and O atoms to the tube are shown in Figs. S3–S5 in Supplementary material in which the HOMO and LUMO plots of pristine and OS-doped SWCNT are displayed in Fig. 4. For single CO molecule adsorbed on pristine SWCNT (Fig. S3), the electron clouds of HOMO and LUMO orbitals are localized surrounding the tube. As the HOMO and LUMO orbitals of CO molecule adsorbed on pristine SWCNT are located at the same regions, these limit the charge transfer to a certain extent. For the CO molecule adsorbed on TM-doped SWCNT systems, most of the electron clouds of HOMO are mainly located on adsorption site which provide electrons in the adsorption process. Whereas, the LUMO orbitals are also localized around the adsorption site and some surrounding CO molecule which get electrons in adsorption process suggesting that the electrons conduct through this system. These suggest that the charge transfers between TM-SWCNT and CO molecules. At the same time, it also shows that there is an obvious hybrid phenomenon between doping area of TM-doped SWCNT and CO molecule which is consistent with the above analysis. This is in good agreement with previous literature [56]. The localization of electron clouds of HOMO and LUMO orbitals appeared around the adsorption site, and gas molecule confirms the strong interaction between gas molecule and TM-doped

nanostructure. The calculated results are well consistent with previous literatures and indicate the improved sensing performance of TM-doped nanostructure to gas molecule [57–59].

In order to explore the effect of CO adsorption to electronic structures of SWCNT, the DOS plots of single and multiple CO molecules adsorbed on pristine, Fe-, Ru-, and Os-doped SWCNT were investigated (Figs. S1, S5, and S6 in

**Fig. 5** DOS of (a) CO/SWCNT, (b) CO/SWCNT, (c) CO/Os-SWCNT, (d) CO/Os-SWCNT, (e) 2CO/Os-SWCNT, (f) 2CO/SWCNT, (g) 3CO/Os-SWCNT, and (h) 3CO/Os-SWCNT systems. Black and red lines are before and after CO adsorption, respectively



Supplementary data). The results show that the DOSs of the pristine SWCNT and its CO adsorption are similar due to very small charge transfer and very weak interaction between CO molecules and pristine SWCNT. While the DOSs of Fe-, Ru-, and Os-doped SWCNT are clearly different from their CO adsorptions indicating that TM-doped SWCNT displays strong interaction to CO molecule. Besides, the DOSs of single and multiple CO molecules adsorbed on TM-doped SWCNT by C atom pointing to tube are more significantly changed than that of O atom in which Os-SWCNT displays the significantly changed (Fig. 5). According to large charge, transfer mainly occurs from the CO molecule to the TM-doped SWCNT. The energy level of HOMO and LUMO and energy gap are changed revealing that CO adsorption changes the DOS of TM-doped SWCNT system. On the one hand, there exists the clearly change of the electronic property of TM-doped SWCNT due to CO adsorption [33].

It can be summarized here that after CO adsorption on TM-doped SWCNT, the DOS and HOMO–LUMO plots and energy gaps of TM-doped SWCNT have much notable change. These are an evidence of the strong interaction between CO molecule and TM-doped SWCNT. In other words, the adsorption of the gas molecule on nanostructure could considerably change the electrical properties of the nanostructure, and this change can be used as a sign in designing an electronic-based sensor for detection and sensing [60, 61].

## Conclusions

The CO molecule is a kind of harmful gas produced in the process of many industries. Single-wall carbon nanotube is a widely used adsorbent material. The adsorption behavior of CO molecule adsorbed on the pristine, Fe-, Ru-, and Os-doped SWCNT was investigated using the first-principles density functional theory. The results show that the transition metal doping on SWCNT can improve the adsorption ability of SWCNT to CO molecule in which the adsorption ability of TM-doped SWCNT is higher than that of pristine SWCNT. When considering adsorption ability of pointing configurations of C and O atoms of CO to the TM-doped SWCNT, the system of pointing C atom of single CO molecule to the Os-doped SWCNT is found to be the most stable configuration, whereas the system of pointing O atom of single CO molecule to the Fe-doped SWCNT is the most stable configuration. The Os-doped SWCNT also displays the strong interaction with two and three CO molecules. The energetically feasibility of adsorption process depends on the structures of the surrounding bonds of the adsorbing atoms plus SWCNT-carbon hybridization and electron transfer from CO to TM-SWCNT. The HOMO, LUMO, and DOS plots of TM-doped SWCNT display a clear change of the electronic properties of TM-SWCNT due to CO adsorption. Therefore, this study may

provide new insight to CO gas-sensing and monitoring nanotechnology, and the results may provide theoretical guidance for higher CO storage capability.

**Acknowledgments** The authors gratefully acknowledge the Computational Chemistry Center for Nanotechnology (CCCN), Department of Chemistry, Faculty of Science and Technology, and Research and Development Institute, Rajabhat Maha Sarakham University, for the facilities provided.

**Funding information** Our gratitude extends to Supramolecular Chemistry Research Unit (SCRU) and the Postgraduate Education and Research in Chemistry (PERCH–CIC) program in the Department of Chemistry, Faculty of Science, Mahasarakham University, for partial financial support.

## References

1. Klabunde KJ, Richards RM (2009) Nanoscale materials in chemistry. John Wiley & Sons, Inc., Hoboken
2. Gong JR (2011) SWCNT–synthesis, characterization, properties and applications. InTech, Inc., Rijeka
3. Mikhailov S (2011) Physics and applications of SWCNT–theory. InTech, Inc., Rijeka
4. Kharlamova MV (2016) Advances in tailoring the electronic properties of single-walled carbon nanotubes. *Prog Mater Sci* 77:125–211
5. Kong L, Enders A, Rahman TS, Dowben PA (2014) Molecular adsorption on graphene. *J Phys Condens Matter* 26:443001
6. Fowler JD, Allen MJ, Tung VC, Yang Y, Kaner RB, Weiller BH (2009) Practical chemical sensors from chemically derived SWCNT. *ACS Nano* 3:301–306
7. Zhang YH, Chen YB, Zhou KG, Liu CH, Zeng J, Zhang HL, Peng Y (2009) Improving gas sensing properties of SWCNT by introducing dopants and defects: a first-principles study. *Nanotechnology* 20(18):185504
8. Iijima S, Ichihashi T (1993) Single-shell carbon nanotubes of 1–nm diameter. *Nature* 363:603–605
9. Zaporotskova IV, Boroznina NP, Parkhomenko YN, Kozhitov LV (2016) Carbon nanotubes: sensor properties. A review. *Mod Electron Mater* 2:95–105
10. Llobet E (2013) Gas sensors using carbon nanomaterials: a review. *Sensors Actuators B Chem* 179:32–45
11. Dai J, Yuan J, Giannozzi P (2009) Gas adsorption on SWCNT doped with B, N, Al, and S: a theoretical study. *Appl Phys Lett* 95:232105–232107
12. Yoon HJ, Jun DH, Yang JH, Zhou Z, Yang SS, Cheng MMC (2011) Carbon dioxide gas sensor using a SWCNT sheet. *Sensors Actuators B Chem* 157:310–313
13. Zhao JX, Chen Y, Fu HG (2012) Si–embedded graphene: an efficient and metal-free catalyst for CO oxidation by N<sub>2</sub>O or O<sub>2</sub>. *Theor Chem Accounts* 131:1242
14. Azizi K, Hashemianzadeh SM, Bahramifar S (2011) Density functional theory study of carbon monoxide adsorption on the inside and outside of the armchair single-walled carbon nanotubes. *Curr Appl Phys* 11:776–782
15. Kong J, Chapline MG, Dai HJ (2001) Functionalized carbon nanotubes for molecular hydrogen sensors. *Adv Mater* 13:1384–1386

16. Peng S, Cho K (2003) *Ab initio* study of doped carbon nanotube sensors. *Nano Lett* 3:513–517
17. Zhang X, Gong X (2015) DFT, QTAIM, and NBO investigations of the ability of the Fe or Ni doped CNT to absorb and sense CO and NO. *J Mol Model* 21:225
18. Li KJ, Wang WC, Cao DP (2011) Metal (Pd, Pt)-decorated carbon nanotubes for CO and NO sensing. *Sensors Actuators B Chem* 159:171–177
19. Yoosefian M, Barzgar Z, Yoosefian J (2014) *Ab initio* study of Pd-decorated single-walled carbon nanotube with C-vacancy as CO sensor. *Struct Chem* 25:9–19
20. Yoosefian M, Zahedi M, Mola A, Naserian S (2015) A DFT comparative study of single and double SO<sub>2</sub> adsorption on Pt-doped and Au-doped single-walled carbon nanotube. *Appl Surf Sci* 349:864–869
21. Ngwashi DK (2010) *Ab initio* investigation of oxygen adsorption on the stability of carbon nanotube field effect transistors (CNTFETs). *Solid State Commun* 150:258–261
22. Azizi K, Karimpanah M (2013) Computational study of Al- or P-doped single-walled carbon nanotubes as NH<sub>3</sub> and NO<sub>2</sub> sensors. *Appl Surf Sci* 285P:102–109
23. Tabtimisai C, Wannu B, Ruangpornvisuti V (2013) Theoretical investigation of CO<sub>2</sub> and NO<sub>2</sub> adsorption onto Co-, Rh- and Ir-doped (5,5) single-walled carbon nanotubes. *Mater Chem Phys* 138:709–715
24. Zhou Q, Wang C, Fu Z, Zhang H, Tang Y (2014) Adsorption of formaldehyde molecule on Al-doped vacancy-defected single-walled carbon nanotubes: a theoretical study. *Comput Mater Sci* 82:337–344
25. Zhang X, Cui H, Chen D, Dong X, Tang J (2018) Electronic structure and H<sub>2</sub>S adsorption property of Pt<sub>3</sub> cluster decorated (8,0) SWCNT. *Appl Surf Sci* 428:82–88
26. Aguiar EC, Longo RL, da Silva JBP (2017) Modeling zigzag CNT: dependence of structural and electronic properties on length, and application to encapsulation of HCN and C<sub>2</sub>H<sub>2</sub>. *J Mol Model* 23:144
27. Ernst A, Zibrak JD (1998) Carbon monoxide poisoning. *N Engl J Med* 339:1603–1608
28. Cortés-Arriagada D, Villegas-Escobar N, Ortega DE (2018) Fe-doped graphene nanosheet as an adsorption platform of harmful gas molecules (CO, CO<sub>2</sub>, SO<sub>2</sub> and H<sub>2</sub>S), and the co-adsorption in O<sub>2</sub> environments. *Appl Surf Sci* 427:227–236
29. Wannu B, Tabtimisai C (2014) A DFT investigation of CO adsorption on VIII B transition metal-doped graphene sheets. *Superlattice Microst* 67:110–117
30. Shukri MSM, Saimin MNS, Yaakob MK, Yahya MZA, Taib MFM (2019) Structural and electronic properties of CO and NO gas molecules on Pd-doped vacancy graphene: a first principles study. *Appl Surf Sci* 494:817–828
31. Esrafil MD, Heydari S (2019) B-doped C<sub>3</sub>N monolayer: a robust catalyst for oxidation of carbon monoxide. *Theor Chem Accounts* 138:57
32. Wang R, Zhang D, Sun W, Han Z, Liu C (2007) A novel aluminum-doped carbon nanotubes sensor for carbon monoxide. *J Mol Struct THEOCHEM* 806:93–97
33. Liu Y, Zhang H, Zhang Z, Jia X, An L (2019) CO adsorption on Fe-doped vacancy-defected CNTs – a DFT study. *Chem Phys Lett* 730:316–320
34. Wang Y, Tong YC, Yan PJ, Xu XJ, Li Z (2019) Attachment of CO to a (6, 6) CNT with a Sc adsorbate atom. *Struct Chem* 30:399–408
35. Frisch MJ, Trucks GW, Schlegel HB, Scuseria GE, Robb MA, Cheeseman JR, Montgomery JA, Vreven T, Kudin KN, Burant JC, Millam JM, Lyengar SS, Tomasi J, Barone V, Mennucci B, Cossi M, Scalmani G, Rega N, Petersson GA, Nakatsuji H, Hada M, Ehara M, Toyota K, Fukuda R, Hasegawa J, Ishida M, Nakajima T, Honda Y, Kitao O, Nakai H, Klene M, Li X, Knox JE, Hratchian HP, Cross JB, Adamo C, Jaramillo J, Gomperts R, Stratmann RE, Yazyev O, Austin A, Cammi R, Pomell C, Ochterski JW, Ayala PY, Morokuma K, Voth GA, Salvador P, Dannenberg JJ, Zakrzewski VG, Dapprich A, Daniels AD, Strain MC, Farkas O, Malick DK, Rabuck AD, Raghavachari K, Foresman JB, Ortiz J, Cui Q, Baboul AG, Clifford S, Cioslowski J, Stefanov BB, Liu G, Liashenko A, Piskorz P, Komaromi I, Martin RL, Fox DJ, Keith T, Laham MA, Peng CY, Nanayakkara A, Challacombe M, Gill PM, Johnson B, Chen W, Wong MW, Gonzalez C, Pople JA (2009) GAUSSIAN 09, Revision A.02. Gaussian Inc, Wallingford
36. Becke AD (1988) Density-functional exchange-energy approximation with correct asymptotic behavior. *Phys Rev A* 38:3098–3100
37. Becke AD (1993) Density-functional thermochemistry. III The role of exact exchange. *J Chem Phys* 98:5648–5652
38. Lee C, Yang W, Parr RG (1988) Development of the Colle-Salvetti correlation-energy formula into a functional of the electron density. *Phys Rev B* 37:785–789
39. Hay PJ, Wadt WR (1985) *Ab initio* effective core potentials for molecular calculations. Potentials for the transition metal atoms Sc to Hg. *J Chem Phys* 82:270–283
40. Wadt WR, Hay PJ (1985) *Ab initio* effective core potentials for molecular calculations. Potentials for main group elements Na to Bi. *J Chem Phys* 82:284–298
41. Hay PJ, Wadt WR (1985) *Ab initio* effective core potentials for molecular calculations. Potentials for K to Au including the outermost core orbitals. *J Chem Phys* 82:299–310
42. Montejo-Alvaro F, Oliva J, Herrera-Trejo M, Hdz-García HM, Mtz-Enriquez AI (2019) DFT study of small gas molecules adsorbed on undoped and N-, Si-, B-, and Al-doped graphene quantum dots. *Theor Chem Acc* 138:37
43. Panahi Y, Sadeghi MM (2019) Application of metallofullerene towards adsorption of mustard gas: a detailed DFT study. *J Inorg Organomet Polym Mater* 29:1383–1389
44. Tabtimisai C, Sontua T, Motongsri T, Wannu B (2018) A DFT study of H<sub>2</sub>CO and HCN adsorptions on 3d, 4d, and 5d transition metal-doped graphene nanosheets. *Struct Chem* 29:147–157
45. Flükiger P, Lüthi HP, Portmann S (2000) MOLEKEL 4.3, Swiss center for scientific computing. Manno
46. O'Boyle NM, Tenderholt AL, Langner KM (2008) A library for package-independent computational chemistry algorithms. *J Comput Chem* 29:839–845
47. Odom TW, Huang JL, Kim P, Lieber CM (1998) Atomic structure and electronic properties of single-walled carbon nanotubes. *Nature* 391:62–64
48. Fellah MF (2011) CO and NO adsorptions on different iron sites of Fe-ZSM-5 clusters: a density functional theory study. *J Phys Chem C* 115:1940–1951
49. Lewis SP, Rappe AM (1995) Quantum-mechanical investigation of bonding and vibrational properties of CO-adsorbed copper. *SPIE* 2547:227–239
50. Ao ZM, Li S, Jiang Q (2010) Correlation of the applied electrical field and CO adsorption/desorption behavior on Al-doped graphene. *Solid State Commun* 150:680–683
51. Sun M, Xu JW, Cui Y, Wu GL, Zhang H, Li ZS (2013) Theoretical study of adsorption CO molecule on palladium-doped boron nitride nanotubes. *Adv Mater Res* 662:233–238
52. Pearson RG (1963) Hard and soft acids and bases. *J Am Chem Soc* 85(22):3533–3539
53. Velázquez-López LF, Pacheco-Ortín SM, Mejía-Olvera R, Agacino-Valdés E (2019) DFT study of CO adsorption on nitrogen/boron doped-graphene for sensor applications. *J Mol Model* 25:91
54. Li S (2006) *Semiconductor physical electronics* 2nd edn. Springer, New York

55. Korotcenkov G (2013) Sensing layers in work–function–type gas sensors, in: Handbook of gas sensor materials, Springer, New York
56. Chandiramouli R, Srivastava A, Nagarajan V (2017) First-principles insights of CO adsorption characteristics on Ge and In substituted silicene nanosheet. *Silicon* 9:327–337
57. Ramasami P (2019) Density functional theory: advances in applications. Walter de Gruyter GmbH, Berlin/Boston
58. Zhang X, Tang J, Xiao S, Zeng F, Pan C, Gui Y (2017) Nanomaterials based gas sensors for SF<sub>6</sub> decomposition components detection. Intech, Croatia
59. Saikia N, Deka RC (2013) Density functional study on the adsorption of the drug isoniazid onto pristine and B-doped single wall carbon nanotubes. *J Mol Model* 19:215–226
60. Chen W, Tang Y, Zhao G, Teng D, Chai H, Feng Z, Dai X (2020) Gas adsorption induces the electronic and magnetic properties of metal modified divacancy graphene. *J Phys Chem Solids* 136: 109151
61. Dutta A, Pradhan AK, Qi F, Mondal P (2020) Computation-led design of pollutant gas sensors with bare and carbon nanotube supported rhodium alloys. *Monatsh Chem* 151:159–171

**Publisher's note** Springer Nature remains neutral with regard to jurisdictional claims in published maps and institutional affiliations.